batteries

MDPI

Article

One-Dimensional Electro-Thermal Modelling of Battery Pack Cooling System for Heavy-Duty Truck Application

Mateusz Maciocha [1], Thomas Short [1], Udayraj Thorat [1], Farhad Salek [2], Harvey Thompson [1] and Meisam Babaie [1,*]

[1] School of Mechanical Engineering, University of Leeds, Leeds LS2 9JT, UK; u.y.thorat@leeds.ac.uk (U.T.); h.m.thompson@leeds.ac.uk (H.T.)
[2] AVL Powertrain UK LTD, Coventry CV4 7EZ, UK; farhad.salek@avl.com
* Correspondence: m.babaie@leeds.ac.uk

Abstract: The transport sector is responsible for nearly a quarter of global CO_2 emissions annually, underscoring the urgent need for cleaner, more sustainable alternatives such as electric vehicles (EVs). However, the electrification of heavy goods vehicles (HGVs) has been slow due to the substantial power and battery capacity required to match the large payloads and extended operational ranges. This study addresses the research gap in battery pack design for commercial HGVs by investigating the electrical and thermal behaviour of a novel battery pack configuration using an electro-thermal model based on the equivalent circuit model (ECM). Through computationally efficient 1D modelling, this study evaluates critical factors such as cycle ageing, state of charge (SoC), and their impact on the battery's range, initially estimated at 285 km. The findings of this study suggest that optimal cooling system parameters, including a flow rate of 18 LPM (litres per minute) and actively controlling the inlet temperature within ±7.8 °C, significantly enhance thermal performance and stability. This comprehensive electro-thermal assessment and the advanced cooling strategy set this work apart from previous studies centred on smaller EV applications. The findings provide a foundation for future research into battery thermal management system (BTMS) design and optimised charging strategies, both of which are essential for accelerating the industrial deployment of electrified HGVs.

Keywords: driving cycle; electric truck; dynamic battery thermal model; BTMS; equivalent circuit model

Academic Editor: Rodolfo Dufo-López

Received: 5 December 2024
Revised: 13 January 2025
Accepted: 23 January 2025
Published: 31 January 2025

Citation: Maciocha, M.; Short, T.; Thorat, U.; Salek, F.; Thompson, H.; Babaie, M. One-Dimensional Electro-Thermal Modelling of Battery Pack Cooling System for Heavy-Duty Truck Application. *Batteries* **2025**, *11*, 55. https://doi.org/10.3390/batteries11020055

1. Introduction

One of the main challenges that the modern world continues to face is climate change and the global warming process associated with it. Global temperatures have increased by more than 1 °C since 1880, with most of this rise occurring since 1975 [1]. The main driver of this continues to be the global production of CO_2, with the transport sector accounting for 24% of the 33.5 billion tonnes produced annually [2]. Having been highlighted as a leading contributor, governments globally have placed stricter emissions legislation on the transport sector. The EU and UK governments have introduced policies to suspend the sale of fossil fuel-powered consumer vehicles beyond 2035 [3,4]. This will leave a void in sales of more than 10 million vehicles annually [5], which will likely be filled by vehicles featuring either electric or hydrogen propulsion systems. In anticipation of the transition to more environmentally friendly vehicles, the popularity of EVs (electric vehicles) has risen exponentially over recent years, with this trend likely to continue [6].

Despite similar legislation [7], the heavy-duty commercial vehicle sector has been slower to electrification than other sectors [8]. As of 2021, only 0.3% of global new truck registrations were attributed to electrically powered vehicles, accounting for less than 0.1% of the total global fleet [9]. The slow transition is likely due to significantly increased payloads [10] requiring advancements in batteries and electric drive units (EDUs).

EDUs capable of supplying the required power for electric heavy-duty trucks have now been developed, which can provide high power such as 375 kW continuously [11]. Despite this, limited research and development have been carried out to enable the production of equally capable battery systems. Where the literature is available, it usually focuses on passenger and light-duty commercial vehicles, hindering heavy-good vehicle electrification [11].

Automobile applications feature significantly more demanding technical requirements than customer electronics regarding capacity, operating temperature range, cost, and cycle life. Mathematical models can predict system characteristics in different environments and conditions, enabling assessment of the performance and range of EVs [12]. Due to the complexity of large-scale energy storage systems and their loading cycles, computational methods are most used for these assessments. Tools such as AVL Cruise and MATLAB Simulink R2023b allow for incorporating vehicle parameters, drive cycle requirements, and battery characteristics through mathematical equations representing physical and chemical reactions [13–15].

Mathematical models estimate the performance of individual cells or whole systems, with SoC, voltage, current draw, and power supply among the parameters of significant interest [15–17]. It is, therefore, essential to model these accurately to ensure physical battery operation is as predicted, as this allows manufacturers to establish whether performance targets can be met reliably and safely by the system. The ability to mathematically model lithium-ion (Li-ion) batteries is vital for the development of battery management systems (BMS), which help to maintain electrical and thermal balance in energy storage systems (ESS) [18].

Effective Battery Thermal Management Systems (BTMS) are needed within EV battery packs as Li-ion batteries' performance and safety characteristics are sensitive to cell temperatures [18]. It is generally accepted that Li-ion batteries tend to perform optimally between 25 °C and 35 °C [19,20]. Above this range, the cycle life of Li-ion batteries tends to decrease exponentially. Tarascone et al. [21] found that in early rechargeable Li-ion batteries, the battery cycle life at 25 °C was approximately 250% greater than that at 55 °C. Similar harmful impacts on Li-ion cell capacity have been found below optimal temperatures, with Lo [22] showing up to 30% reductions in cell capacity at −20 °C. Temperature differences within Li-ion cells and across battery packs have also been found to hinder overall performance. It has been suggested that a maximum difference of 5 °C should not be exceeded within cells and between modules to maintain optimal performance [23,24] and avoid potential short-circuiting [25]. Temperature differences more significant than this have increased thermal ageing by 25% and decreased power capabilities by 10% [26]. Based on existing studies, it can therefore be suggested that the BTMS must maintain optimal battery temperature (25–35 °C), with a pack temperature range of <5 °C.

Key thermal challenges facing the electrification of HGVs stem from the increased mass and power requirements compared to typical EVs. Typical EVs have masses of around 1600–2300 kg [27,28] and electric drive units capable of supplying 100–150 kW [28]. Due to payloads of up to 44 tonnes, HGVs require motors that can provide high power and torque to perform similarly to current diesel powertrains [29]. The additional mass of loaded HGVs means they can require upwards of 1000% more torque during standardised drive cycles than typical EVs [30–32], thus drawing proportionately more current from

the battery pack. With total heat generation within Li-ion battery systems proportional to the amperage draw squared [24], the increased torque requirements mean that the heat generation per battery cell could be exponentially more significant in electric HGVs than typical EVs, increasing demand on the BTMS. Electric HGVs' more significant power requirements also mean they will likely have much larger battery systems than typical EVs. Typical EVs feature battery capacities of around 40–80 kWh [28], compared to an electric HGV requirement of upwards of 400 kWh [33], to achieve ranges competitive with existing diesel counterparts. At the same current draw, this may mean that the electric truck's total battery heat generation could be up to 750% greater than typical EVs. To maintain thermal stability within the battery, the truck's BTMS and cooling capacity would need to be upscaled sufficiently, with components such as the radiator, compressor, and pumps capable of generating increased heat.

According to Pesaran [34], EV BTMS should use minimal parasitic power while allowing pack operation in hot and cold climates. Potential BTMS designs for typical EVs have been compared in studies, with liquid water/glycol cooling widely regarded as preferential [35]. This has been attributed to the more significant heat transfer coefficients of liquid systems, which can be more than 3× those of equivalent air systems [34]. Such liquid BTMSs can be cooled passively and actively, as detailed by Piao et al. [36], with passive systems only found to be viable for climates between 10 °C and 35 °C [34].

The existing literature has widely studied potential liquid BTMS for consumer EVs, with the inlet temperature and coolant flow rate having been found to play critical roles. Lan et al. [37] studied the effect of coolant flow rate and detailed battery cell thermal behaviour at different C-rates. It was found that an increase in coolant flow rate provided increased cooling across all C-rates but would eventually suffer from diminishing returns. Karimi et al. [38] carried out similar work and achieved flow rate results identical to those of Lan et al. [37], but also studied the effect of inlet temperature on cell temperature. It was shown that a decrease in inlet temperature proportionately decreased maximal cell temperature across the whole battery discharging cycle. For example, at the end of the 1400 s cycle, each 1 °C reduction in coolant inlet temperature reduced the maximal end temperature by 0.6 °C. This trend was repeated across all inlet temperatures. Yue et al. [39] also found similar results at the pack level. These studies suggest that increased coolant flow rate and low coolant inlet temperatures would provide preferential cooling for electric HGV TMS. However, the diminishing returns shown by increased flow rates and the increased energy consumption required for active cooling suggest that both properties should be optimised for each application.

This study addresses these challenges by employing a 1D electro-thermal model within the MATLAB Simulink R2023b environment to assess a potential battery design's electrical and thermal performance for heavy-duty vehicles. This model is based on realistic cell characteristics, real-world power demand data, and driving cycle data for HGVs. Using a 1D model offers a practical solution by increasing the speed and reducing the costs of large-scale simulations while maintaining accuracy. Unlike previous research, this study integrates real-world power demand and drive cycle data for heavy-duty trucks. It also employs realistic cell characteristics and cooling system performance, ensuring the results apply to industrial-scale deployments. An equivalent circuit model (ECM) is calibrated for electro-thermal analysis using actual battery test data. This enhances the reliability of the simulation results, allowing for precise evaluation of battery behaviour under various operating conditions [40].

The primary novel contributions of the present research are as follows:

1. Thermal management solutions for heavy-duty electric vehicles, providing analysis of these vehicles' thermal behaviour.
2. Use of actual drive cycle and power demand data for realistic battery design.
3. The 1D electro-thermal modelling is based on ECM, battery test data, and typical thermal management materials.
4. Industrial-scale applicability using realistic cell characteristics and cooling system performance.

The structure of this paper is as follows: Section 2 outlines the methodology, covering the system description, electrical battery model, and thermal cooling model. Section 3 presents the study's findings, while Section 4 provides an in-depth discussion. Finally, Section 5 concludes with a summary of the key insights.

2. Materials and Methods

2.1. System Description

Prior to the modelling procedure, a battery pack design for an electric heavy-duty truck was created based on typical EV battery specifications and space availability in heavy-duty trucks. Samsung SDI 94 Ah cells [41] were selected for use in the battery pack design due to their suitability in automotive applications, historically proven by their presence in multiple EVs. These cells use lithium-ion chemistry, with a Nickel–Cobalt–Manganese (NMC)-based cathode composition ($Ni_{0.33}Mn_{0.33}Co_{0.33}O_2$) [42].

Following a review of the limited EV trucks available from large original equipment manufacturers (OEMs) [43], minimum electrical capabilities of the novel battery pack were established, with an excess of 600 V and 516 kWh required. Table 1 highlights the battery's electrical architecture, with Table 2 highlighting the system's electrical characteristics.

Table 1. Battery architecture used in the current study.

Type	Module	Pack	Total
Electrical architecture	12 cells in series (12 s)	16 modules in series	7 packs in parallel

Table 2. Battery system parameters used in the current study.

	Cell [41]	Module	Pack	Total
Nominal voltage (V)	3.68	44.16	706.56	706.56
Maximum voltage (V)	4.15	49.80	796.80	796.80
Capacity (Ah)	94	94	94	658
Energy capacity (kWh)	0.35	66.41	64.41	464.92
Maximum energy capacity (kWh)	0.39	74.52	74.52	521.64
Mass (kg)	2.1	28	448	3136

At the point of concept, consideration was made to the spatial requirements of such a battery to allow for its potential future integration into an HGV. An example of the novel battery in situ is shown by 3D visualisation in Figure 1. Prior work has shown that a cooling channel design is the most appropriate for a vehicle of this scale when considering cooling performance, pressure loss, and special requirements [44]. The cooling system was assumed to feature 6 cooling channels per pack, as shown in Figure 2, while using an industry-standard 50:50 water/glycol coolant mixture [45].

Figure 1. Rendering of the battery pack in the truck with and without aero covers.

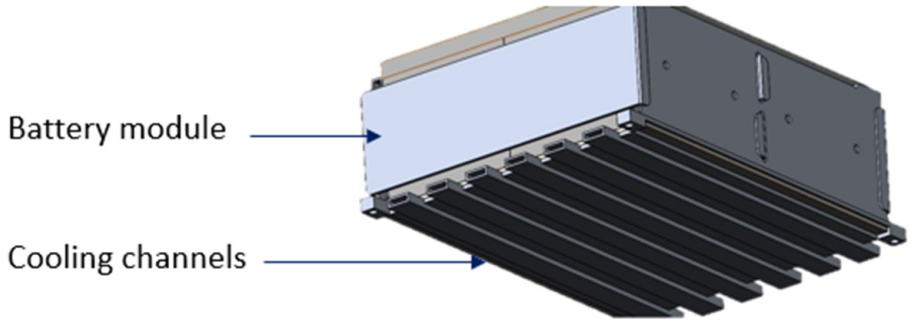

Figure 2. 3D CAD model of battery module with cooling channels.

2.2. Battery Thermal Model

2.2.1. Battery Life Cycle Dynamics and Electrical Parameters Overview

Physical testing data of typical EV battery modules containing Samsung SDI prismatic cells was used to understand cell cycle ageing, with the results summarised in Table 3. The study considered 2000 and 4000 cycles, corresponding to 100%, 90%, and 80% of the state of health (SoH). Further cycle ageing was not considered due to the cell's end of life (EOL) being exceeded, with a replacement expected when the SoH of the cells depletes beyond 80%.

Table 3. Battery life cycle values of a typical EV battery module.

Charge/Discharge Cycles	Capacity Difference at 25 °C (%)	Internal Resistance Difference at 25 °C (%)
1	0	0
2000	−9.96	17.28
4000	−20.28	42.45

Key battery parameters were parametrised within the script and applied to each cell in line with manufacturer datasheets and experimental fade data. The complete block diagram of the electrical system, alongside charge/discharge application and battery performance assessment methods, is also presented in Figure 3. The power demand for each cycle was proportioned to each pack. This meant that including all 7 packs was optional, helping simplify the model while significantly decreasing the computational power without compromising accuracy. Uniform discharge and health degradation were assumed for all the cells in the system; hence, a SoC reading from the output of a single cell was considered sufficient. In the initial stage, the thermal implications were neglected, with perfect cooling assumed, therefore maintaining the cells' temperature at 298.15 K. The electrical model would later be combined with the thermal model to investigate the thermal impacts of varying power demand. Similarly, no self-discharge or memory effect was considered for the cells.

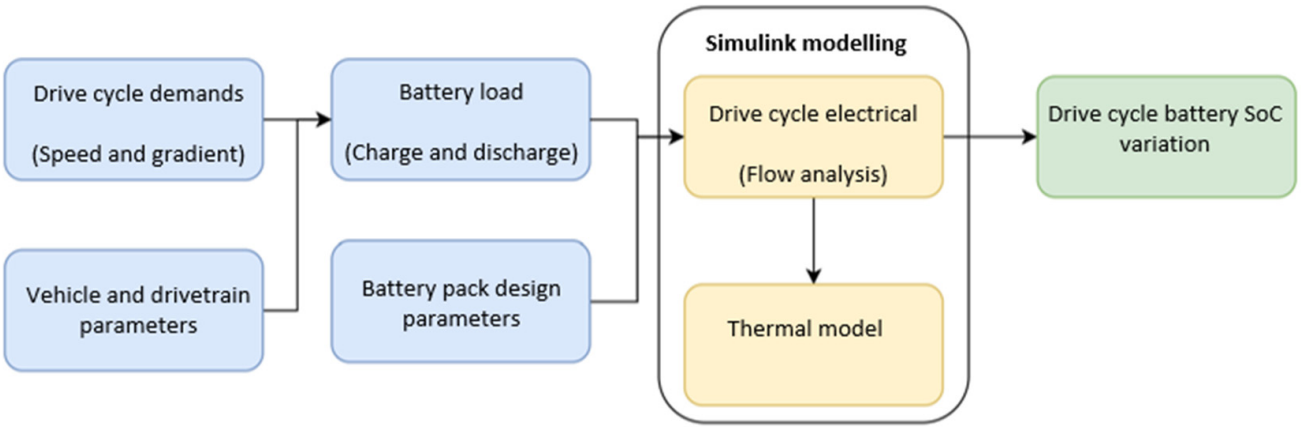

Figure 3. Electrical battery model design (inputs, modelling, and output).

During simulation, the cells' dynamic charge and discharge models were used to determine the cell terminal voltage based on current draw and time. Hence, the depth of discharge provided was defined by Equations (1) and (2), respectively. These models are pre-determined within MATLAB R2023b to suit a lithium-ion type battery, such as the cells used for this paper [46]. Table 4 shows the parameters used in the electrical model.

$$f_c(it,\ i*,\ i) = E_0 - K\left(\frac{Q}{it + 0.1Q}\right) i* - K\left(\frac{Q}{Q - it}\right) it + Ae^{-Bit} \quad (1)$$

$$f_d(it,\ i*,\ i) = E_0 - K\left(\frac{Q}{Q - it}\right) i* - K\left(\frac{Q}{Q - it}\right) it + Ae^{-Bit} \quad (2)$$

Table 4. Parameters of the electrical model.

Parameter	Symbol	Unit
Voltage	E_0	V
Polarisation constant	K	V/Ah
Current dynamics	$i*$	A
Battery current	i	A
Extracted capacity	it	Ah
Maximum battery capacity	Q	Ah
Exponential voltage	A	V
Exponential capacity	B	Ah^{-1}

2.2.2. Equivalent Circuit Model (ECM)

Methods of battery modelling can be split into two main categories, one being the electrochemical models (EM), and the second being the equivalent circuit model (ECM). The ECM utilises components like resistors, capacitors, and voltage sources to form a circuit network that replicates the behaviour and dynamics of a battery [47]. On the other hand, the EM provides a more precise depiction by accounting for the underlying electrochemical processes. The ECMs, particularly resistor–capacitor (RC) networks, are frequently used for lithium-ion battery modelling because they effectively capture the battery's dynamic behaviour.

Simulink's Simscape toolbox allowed the electrical system to be modelled using blocks representing various system components. The equivalent circuit model (ECM) implemented using the battery cell block in Simulink can be seen in Figure 4, alongside a schematic diagram.

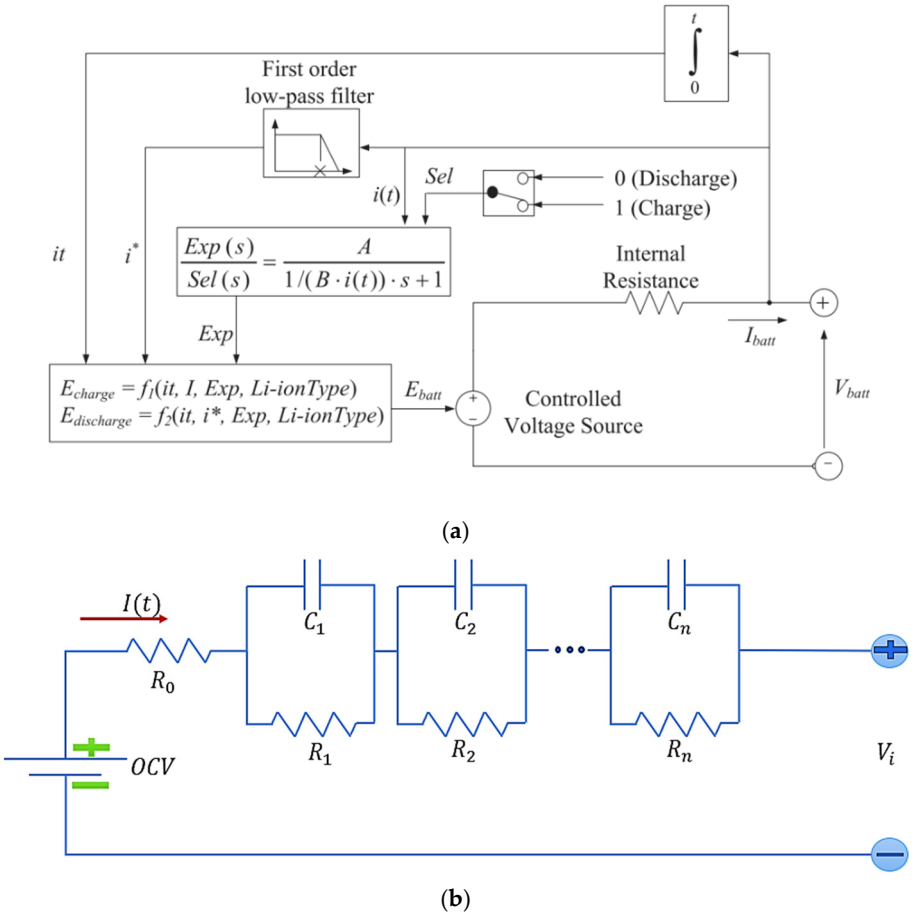

Figure 4. Schematic diagrams: (**a**) equivalent circuit model for Li-ion cell; (**b**) equivalent circuit model of nRC model.

Figure 4b illustrates a standard ECM configuration, specifically, the nRC model, which consists of an n-RC network. The battery's output voltage (V_i) depends on various parameters, such as the open circuit voltage (OCV), ohmic resistance (R_0), polarisation resistance (R_i), and the corresponding polarisation capacitance (C_i), as defined in Equation (3).

$$V_i = OCV - I_i\left[R_0 + \sum_{i=1}^{n} R_i\left(1 - e^{-\frac{t}{R_i C_i}}\right)\right] \quad (3)$$

2.2.3. Drive Cycle Energy Demand Analysis

This study considered two drive cycles—VECTO long haul and AVL These were chosen due to their use in the international emission assessment of modern trucks and their accurate representation of a typical heavy-duty truck drive cycle. The long-haul cycle predominantly features steady-state driving with some stop/start instances, similar to what could be expected of a drive along a motorway with moderate traffic. The AVL cycle is twice as long (200 km) and includes no stopping instances, with only some sections of reduced velocity. The AVL cycle, therefore, maintains a higher average velocity through the cycle and can be said to be representative of a drive through a mountainous region with fluctuations in altitude—the velocity and altitude profiles of each cycle can be seen in Figures 5 and 6.

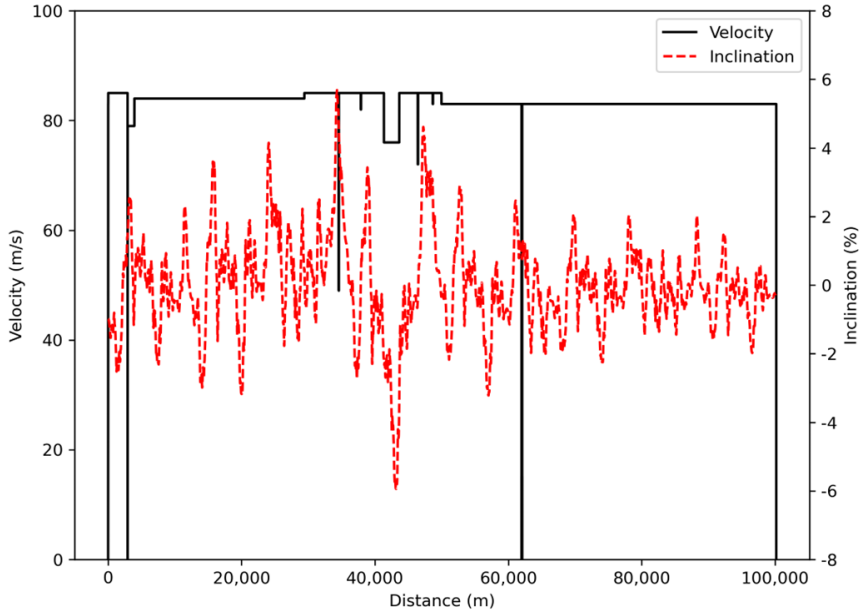

Figure 5. Velocity and inclination profiles for long haul.

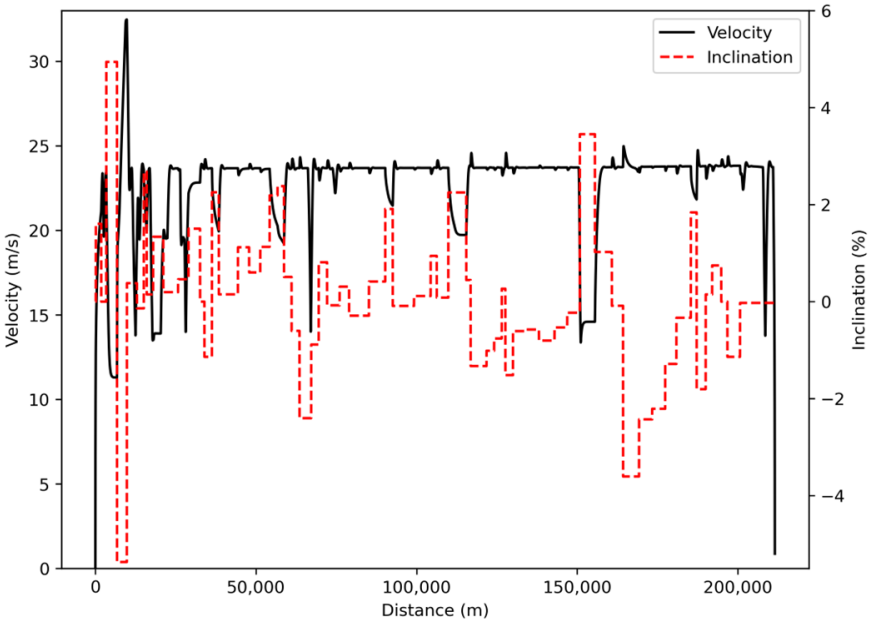

Figure 6. Velocity and inclination profiles for the AVL cycle.

2.3. Thermal Cooling Model

2.3.1. Thermal Parameters Overview

The battery pack materials used during the modelling process were selected based on the previously highlighted battery pack design procedure. The corresponding thermal parameters assumed for the materials were selected based on parameters used typically within existing papers [48–50] and, where available, manufacturer's datasheets. Table 5 provides an overview of the materials. The cooling system parameters were selected similarly, as shown in Table 6.

Table 5. Thermal parameters of the materials used for the battery pack [48–50].

Materials	Thickness (m)	Thermal Conductivity (W/(K∗m))	Application
Aluminium	0.004–0.005	202.40	Cell casing and module plates
HV Insulation	0.002	1.38	Electrical insulation and high-voltage protection
PVC Lid	0.005	0.02	Electrical insulation and thermal protection
Air Pockets	N/A	5.00	Heat Dissipation

Table 6. Cooling system parameters used in the current study [49,51–53].

System	Property	Values
Coolant	Viscosity	4.41 (mPa/s)
	Kinematic Viscosity	4.25 (mm^2/s)
	Thermal Conductivity	0.35 (W/mK)
	Specific Heat Capacity	3.57 (kJ/kg K)
Heat Exchanger Pipes	Thermal Conductivity	202.4 (W/mK)
	Hydraulic Diameter	0.01 (m)
	Pipe Roughness	1×10^{-6} (m)
	Laminar Flow Upper Reynolds Number	2300
	Turbulent Flow Lower Reynolds Number	4000
	Nusselt Number	3.66
	Darcy Friction Factor Constant	64

2.3.2. Simulink Model Overview

Simulink was again used as a simulation environment to model the battery pack and cooling system in 1D, as shown in Figures 7 and 8. The model components were connected electrically and thermally based on the arrangements in Table 5 to produce subsystems of each system level. Each component was assumed to be in contact with surrounding components, except at the pack level, where air spaces were assumed to be surrounding each pack. The battery subsystems were combined to create a representative model of the total battery, as shown in Figure 3.

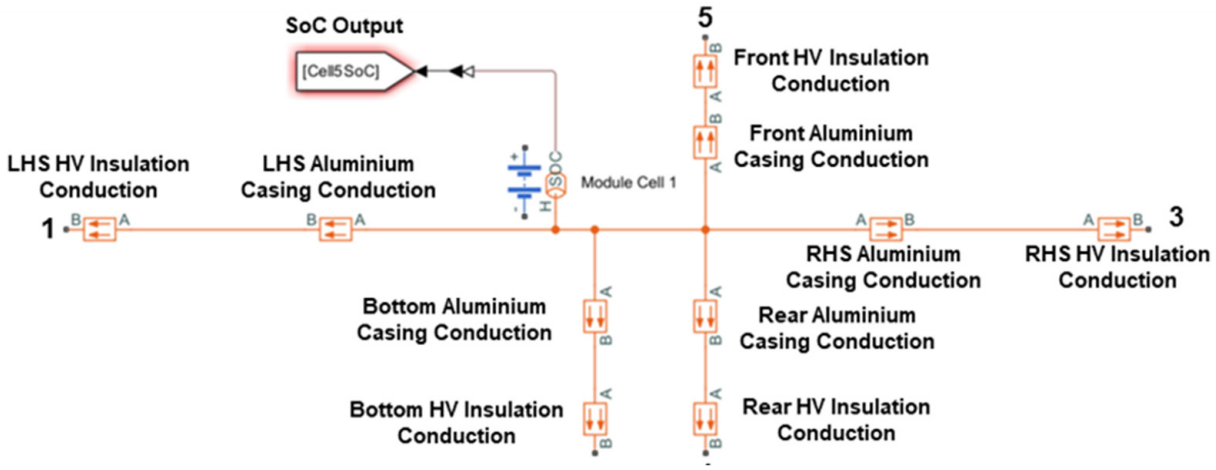

Figure 7. Battery cell thermal model in MATLAB/Simulink R2023b.

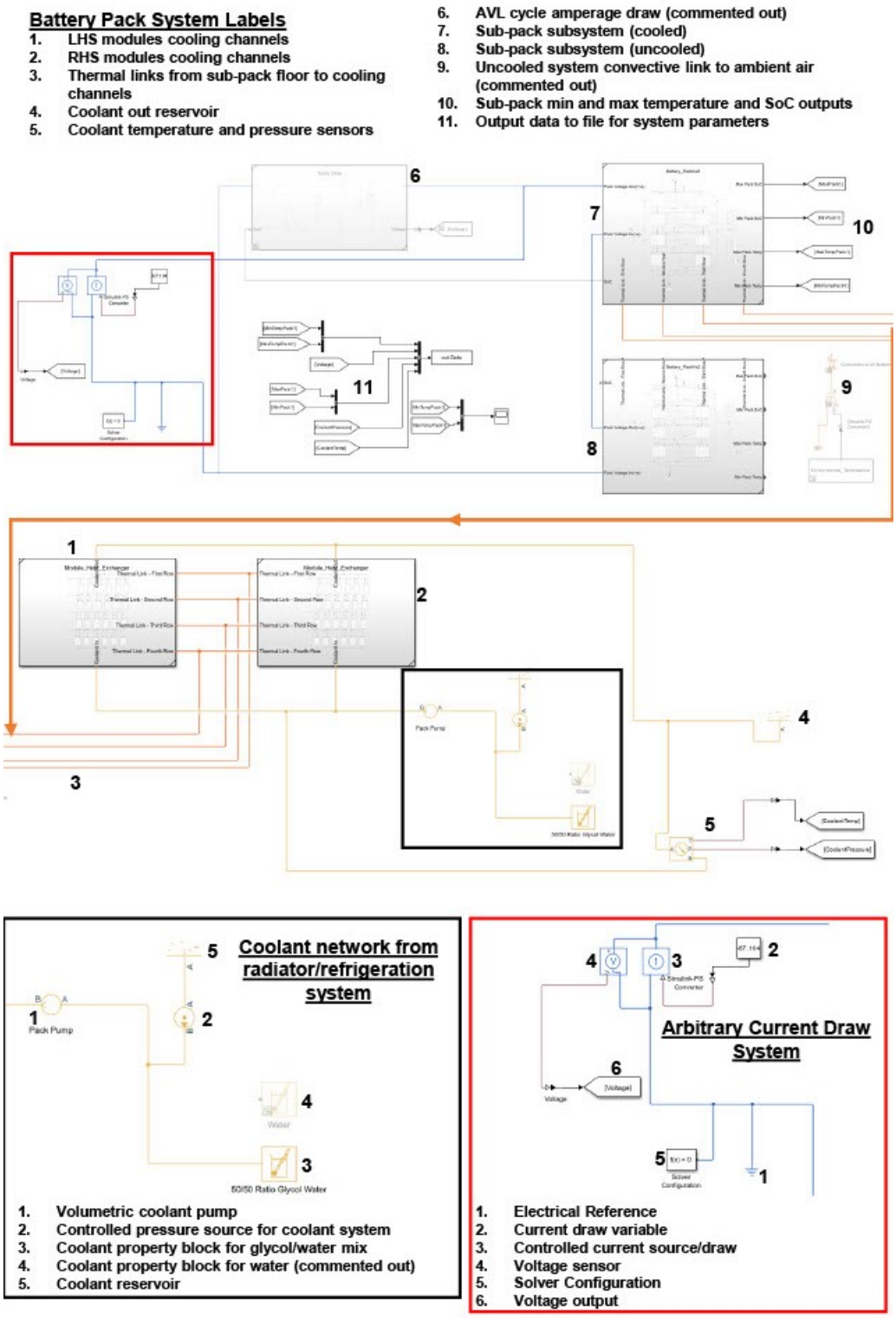

Figure 8. Overview of the 1D electro-thermal Simulink model used in the current study.

2.4. Simplified Assumptions for Battery System Modelling

The electrical battery model assumed uniform discharge, health degradation, and perfect cooling for all cells within the system. Therefore, the cell temperature was considered to be constant at 25 °C in line with the similar existing literature [32]. These assumptions meant that monitoring the electric state of a single cell was assumed sufficient and representative of all cells in the system.

All three models also used one fundamental assumption to reduce computational cost. It was assumed that one pack would provide a representative view of the whole system's behaviour. This was considered valid as the CAD model of the entire system suggested that each pack would be thermally isolated from each other with air. This was implemented by using one pack's cooling system and drawing a power demand for the pack with a scalar equal to $1/7^{th}$ of what would be faced by the total battery pack, therefore reducing computational cost by approximately 86%.

3. Results

3.1. Power Demand

The energy demand for a 44-tonne truck to complete both drive cycles was obtained from simulations carried out in AVL Cruise M, as shown in Figure 9. Both cycles included energy recovery from regenerative braking, as indicated by the positive power demand regions in both figures.

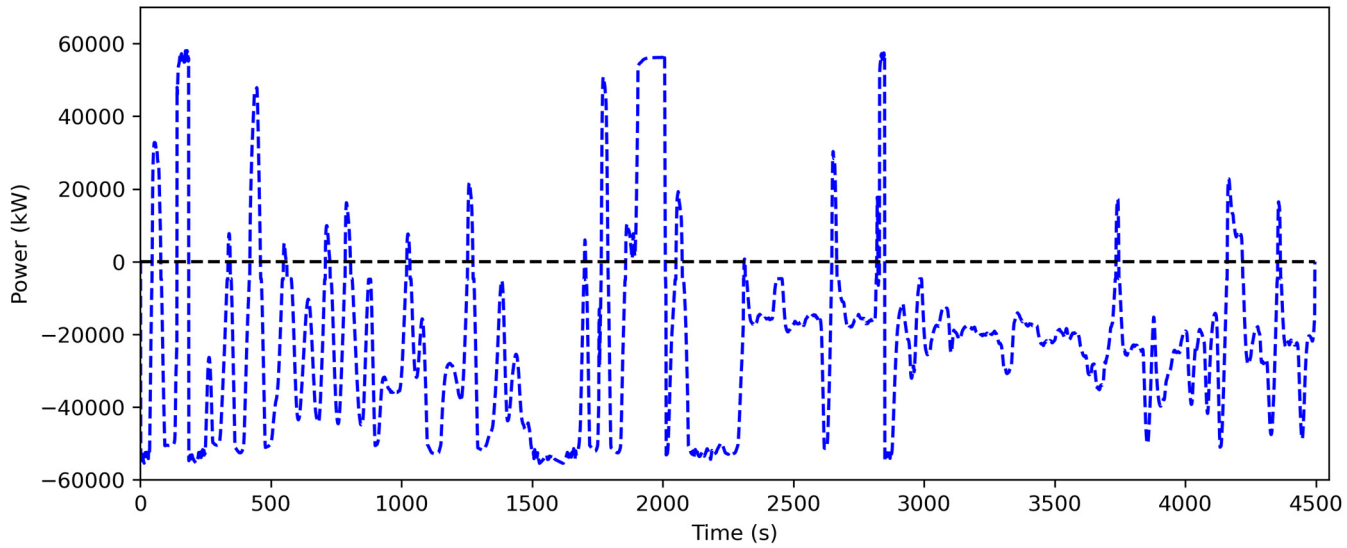

(**a**)

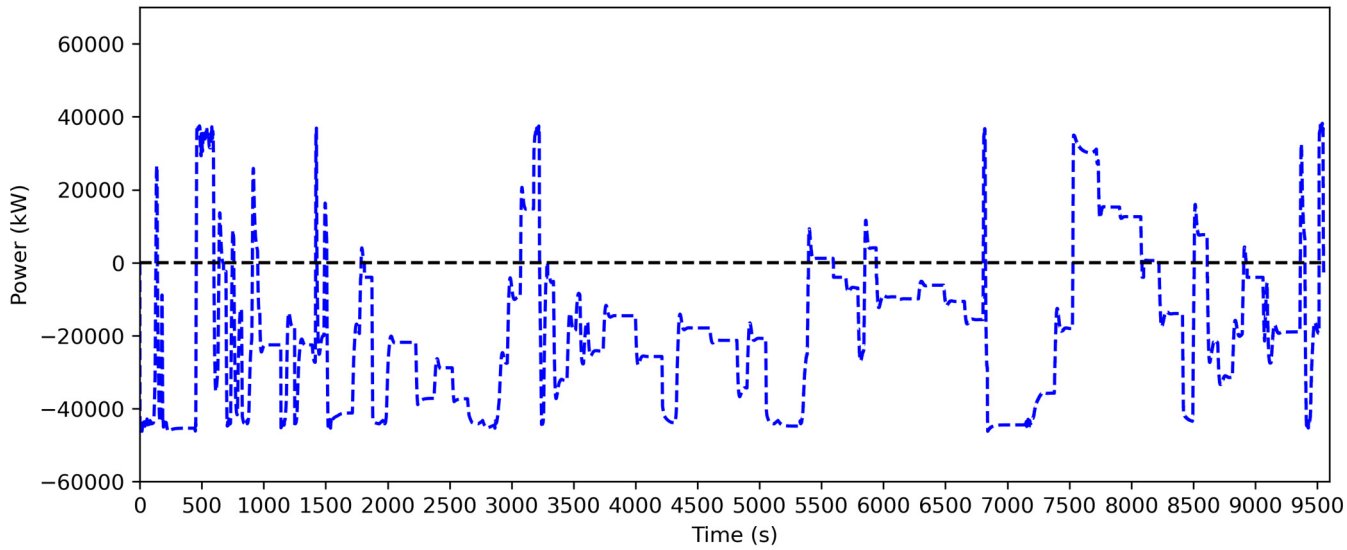

(**b**)

Figure 9. Power demand per pack for (**a**) long-haul cycle, (**b**) AVL cycle.

3.2. Electrical Battery Model

3.2.1. Model Validation

The electrical model was validated by assessing the total power consumption calculated from the initial and final SoC of the battery pack and scaling to consider the full, seven-pack system before comparing it to the literature [54,55]. For validation purposes, the SoH and initial SoC of the cells were taken as 100%. The more significant difference in energy consumption displayed by the long-haul cycle was attributed to the use of different cells in the literature and was therefore ignored. The results from the study can be seen in Table 7; from these, the model was deemed valid.

Table 7. Model simulation results.

Cycles	Energy Consumption—Literature (kWh)	Energy Consumption—Simulink Model (kWh)	Difference (%)
Long-haul	169.42	187.77	10.82
AVL	343.42	339.83	−1.05

3.2.2. Long-Haul Cycle

By varying the initial SoC and SoH values, nine use cases were obtained. The different use cases were investigated for energy consumption and post-cycle SoC, with the results shown below in Table 8 and Figure 10.

Table 8. Results of long-haul cycle.

Cycles	1			2000			4000		
Pack Energy Capacity (kWh)	66.41			59.78			53.13		
Initial SoC	1	0.9	0.8	1	0.9	0.8	1	0.9	0.8
Final SoC	0.60	0.48	0.37	0.55	0.44	0.32	0.48	0.37	0.26
Energy Consumed (kWh)	188	193	197	189	194	199	192	197	201

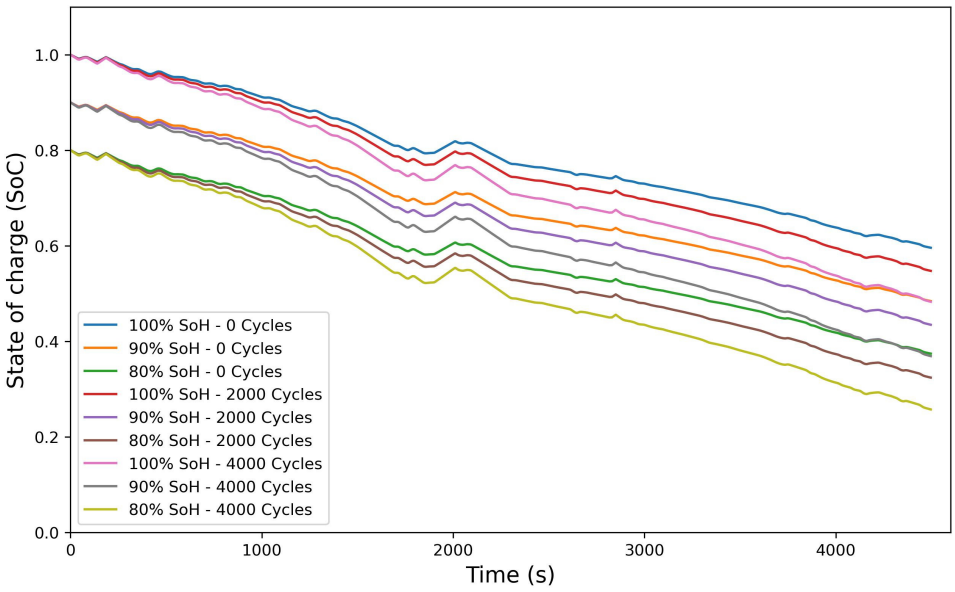

Figure 10. SoC profiles over time for different initial SoC and SoH conditions during long-haul cycle.

3.2.3. AVL Cycle Results

Equivalent use cases to those in Section 3.2.2 were used to analyse the AVL drive cycle for energy consumption and post-cycle SoC. The results are in Table 9 and Figure 11.

Table 9. Results of AVL cycle.

Cycles	1			2000			4000		
Pack Energy Capacity (kWh)	66.41			59.78			53.13		
Initial SoC	1	0.9	0.8	1	0.9	0.8	1	0.9	0.8
Final SoC	0.26	0.18	0.08	0.19	0.11	0	0.09	0	0
Energy Consumed (kWh)	342	333	335	339	331	335	335	335	298

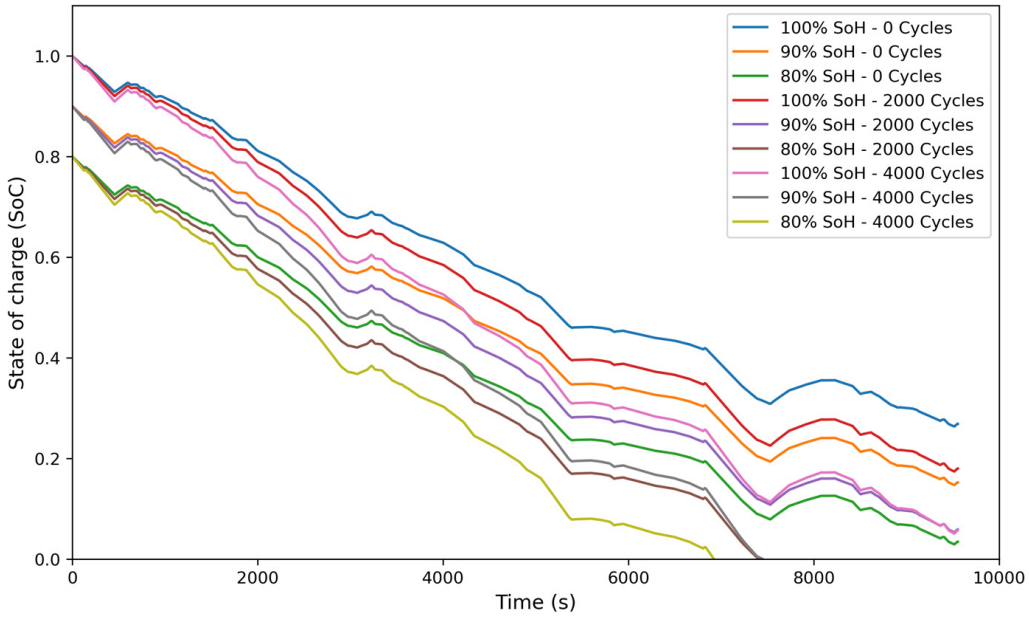

Figure 11. SoC profiles over time for different initial SoC and SoH conditions during AVL Cycle.

3.3. Battery Thermal Management Performance

3.3.1. Flow Rate Simulation Results

The thermal behaviour of the battery pack was simulated for 3600 s at the max C-rates obtained from the AVL cycle. These were 0.714 C and 0.935 C at 100 and 80% battery SoH, respectively, found during the electrical analysis. The median temperature increases and maximum temperature difference over the pack were recorded at varying coolant flow rates. Figures 12 and 13 show the effect of coolant flow rate on temperature increase and difference.

3.3.2. Inlet Simulation Results

The thermal response of the battery pack to varying inlet temperatures was also simulated for 3600 s at 0.714 C. Ambient temperatures of −15 °C, 25 °C and 40 °C were selected to cover both typical ambient temperatures and extremes that the literature has suggested heavy-duty trucks could face [29]. Figures 14 and 15 show how varying the inlet temperature affects battery temperature change.

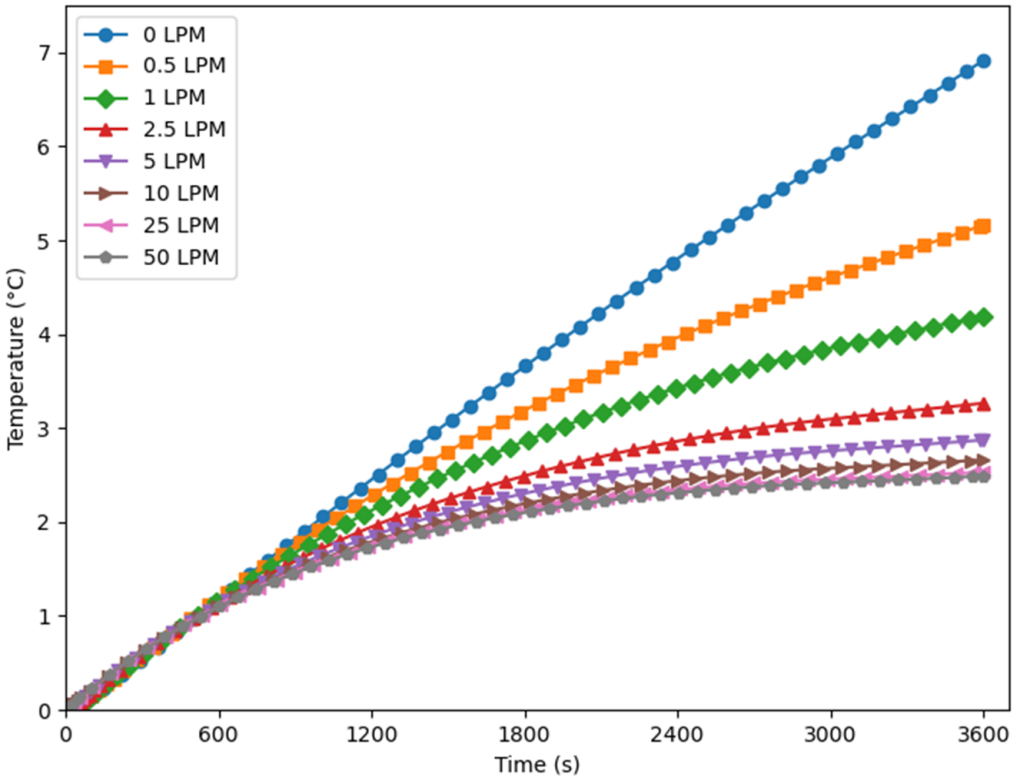

Figure 12. Median temperature increase in the battery pack exposed to 0.714 C at different coolant flow rates.

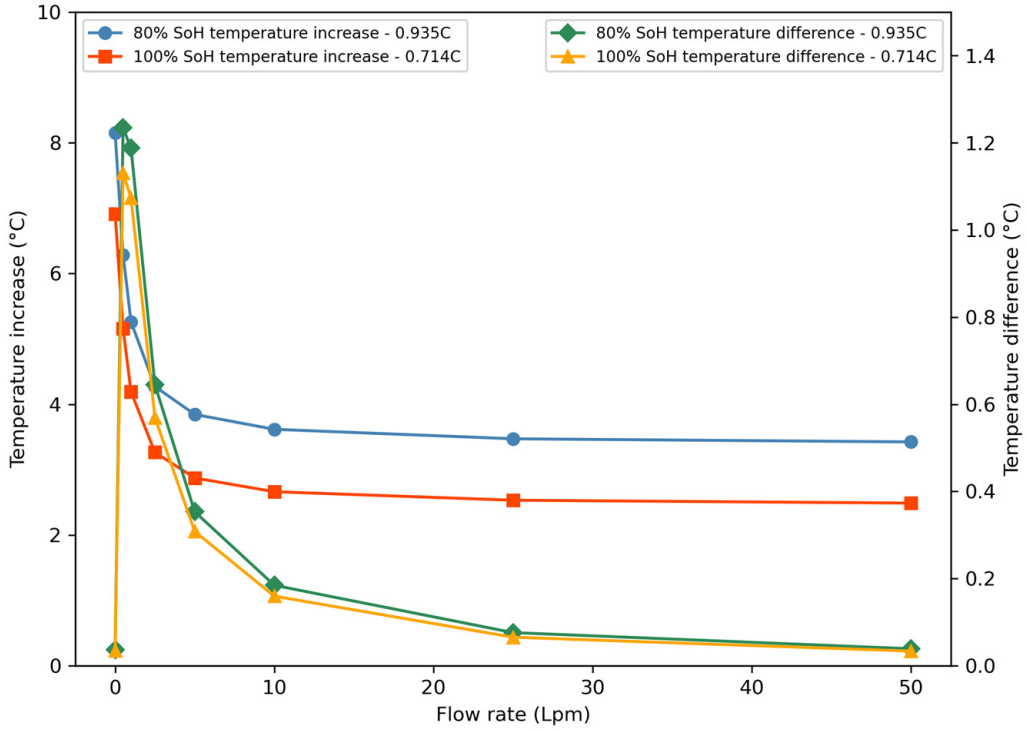

Figure 13. Temperature increase and difference at 3600 s of maximum C-rates from AVL drive cycle.

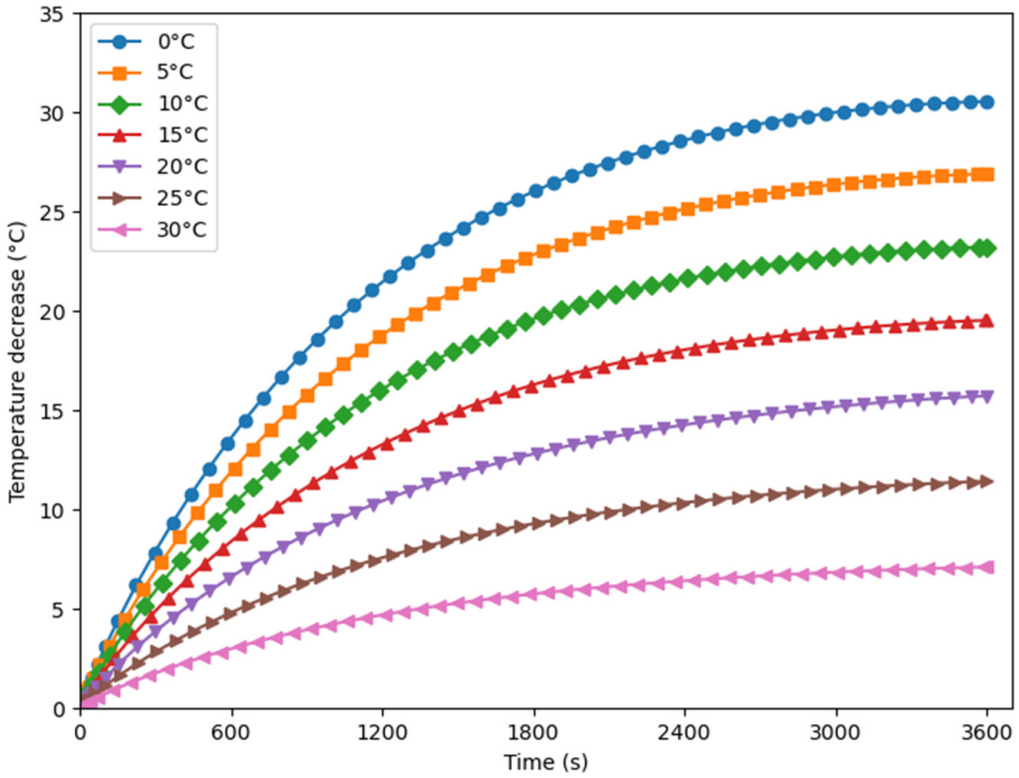

Figure 14. Decrease in temperature of battery pack at varying coolant inlet temperatures at 0.714 C (100% SoH) and 40 °C ambient temperature.

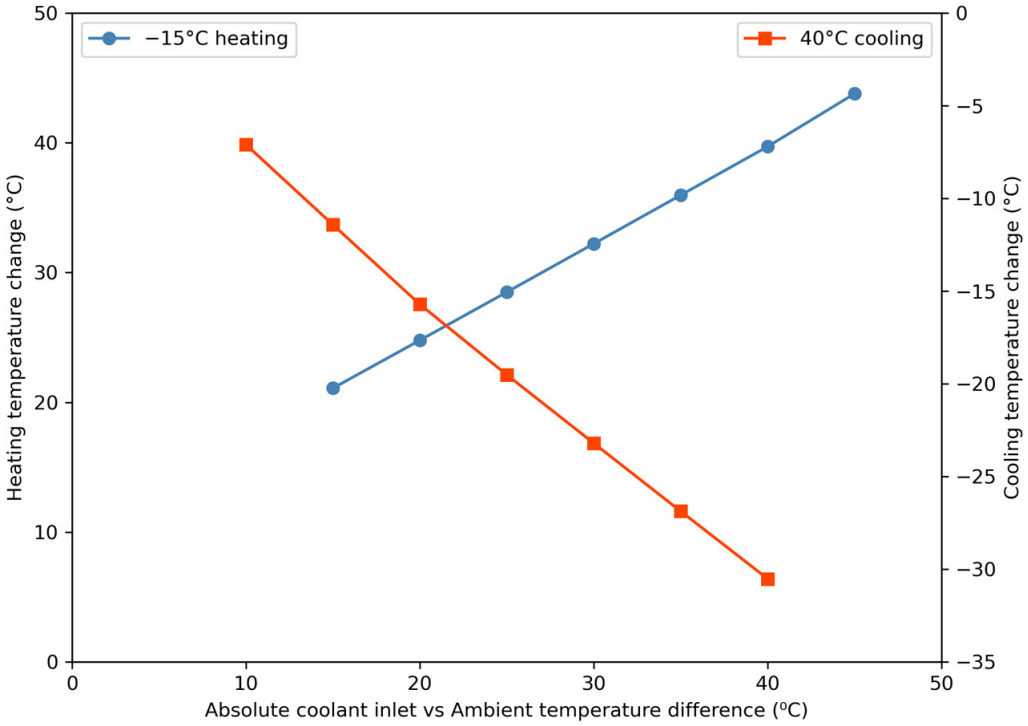

Figure 15. Temperature change in battery pack at varying coolant inlet temperatures at 3600 s of 0.714 C (100% SoH).

3.4. Transient Thermal Performance Analysis of the Battery Pack

Using the optimised BTMS parameters, the thermal behaviour of the truck's battery was analysed under AVL cycle loading at varying ambient temperatures. Each ambient temperature was studied without implementing a cooling system and with predefined optimal coolant parameters. These were determined from the results shown in Section 3.3 for each ambient temperature and can be seen in Table 10. Figure 16 shows the transient analysis results, highlighting the optimal region in grey.

Table 10. Optimised cooling system parameters.

Ambient Temperature (°C)	Coolant Flow Rate (LPM)	Coolant Inlet Temperature (°C)
−15	18	−7.2
25	18	25.0
40	18	32.2

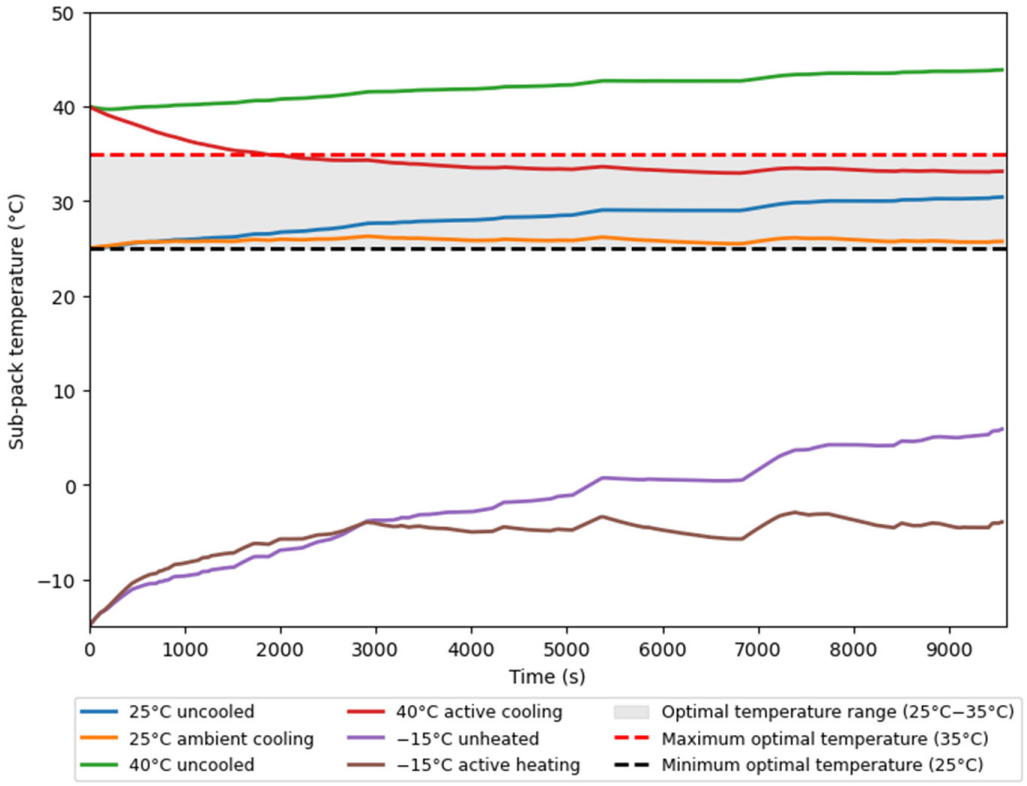

Figure 16. Battery pack temperature during AVL drive cycle loading.

4. Discussion

4.1. Performance Insights from the Electrical Model

4.1.1. Long-Haul Driving Cycle

Based on the post-cycle SoC of the pack, the total energy consumption was calculated to range between 188 and 201 kWh/100 km (~7% range) for the long-haul cycle, as shown in Table 8. This suggests a potential single-charge range of 247 km at full load under optimal operating conditions. As expected, energy consumption for the cycle increased with increased cycle ageing due to the increased internal resistance within each cell. Decreasing the initial SoC also increased energy usage due to the reduced pack voltage. In these scenarios, more current would be drawn to achieve the required power, compensating for the lower voltage. The use case with 100% SoH and SoC appeared to be the most energy

efficient for the cycle, whilst expectedly, the oldest and least charged batteries appeared least efficient.

The final SoC values for the long-haul cycle, as shown in Figure 10, were found to vary from 60% to 26.7%, depending on the initial SoC and SoH. The SoC trend followed expectations from the power demand plot in Figure 9 and showed a steady discharge with one significant section of battery recharge around the 1750 s mark, coinciding with the large, positive peak in the power demand plot. It was also noticed that the power input in the recharge sectors resulted in a higher SoC increase for lower SoH cases. This occurred due to the reduced cell capacity, which allowed for a quicker charge at a constant power input. The impact of the remaining energy recovery sectors (around 200 s and 430 s) was found to be less significant, with the SoC increase not exceeding 1% for all cases. This likely reflects less extreme regenerative braking conditions in which gentle deceleration or less frequent breaking events occurred.

4.1.2. AVL Cycle

Unlike the long-haul cycle, the longer AVL cycle could not be completed in all nine use cases. Table 9 shows the total energy consumption varied between 331 and 342 kWh (3% range) when considering fully completed cycles, suggesting a potential battery range of 285 km under optimal conditions. However, as evident in Table 9, the 100% SoH, SoC battery was found to be the least efficient, contradicting the results from the long-haul cycle. This could be explained by the nature of the route, which contains more areas of regenerative braking, which is potentially more efficient at lower SoHs.

Final SoC values ranged from 26.4% and 0%, with three cases completely discharging the battery before the end of the cycle, as shown in Figure 11. Complete discharge was achieved within the 155 km–165 km range for these cases. The cycle contains three sectors of recharge, with the most significant one occurring around 7500 s. The minimum increase in SoC achieved at this part of the cycle was found to be around 4%. It can be estimated that without this large recharge power peak, a further three cases would not be able to complete the cycle.

4.1.3. Validation of Model

Overall, the model provided energy consumption results, which gave single-charge range predictions in line with current industry standards for electric class eight trucks [56]. The model was also validated by comparing energy consumption with 10.85% and −1.82% difference for the long-haul cycle and AVL cycle, respectively, upon comparison with the literature [56,57], and, hence, high confidence can be placed in the model. The energy flow in the system behaved as expected, showing the expected charge and discharge stages of the pack, accurately reflecting the power draw for each cycle, and giving reliable approximations for variations in SoC.

4.1.4. Key Assumptions and Limitations of the Model

The model utilised three main assumptions: constant temperature, uniform discharge, and uniform cycle ageing of all cells. The validity of these assumptions would be highly dependent on the performance of the cooling and battery management systems, both of which would be required for the battery design to be industrialised.

One modelling assumption that could have compromised the accuracy of results in comparison to experimental data was the neglect of the dynamic constants of the cells. The cells considered in this paper did not undergo characterisation tests, preventing accurate data regarding their behaviour under dynamic loading from being established. Only cycle ageing tests were carried out to understand the cycle ageing implications on the system performance in terms of vehicle single-charge driving range over the lifespan of the pack.

4.2. Thermal Cooling System Model

4.2.1. Coolant Flow Rate

Figures 12 and 13 suggest that with an ambient inlet temperature, cooling performance increases with coolant flow rate, up to a point of diminishing returns. For example, an increase in flow rate from 1 to 10 LPM at 0.714 C decreased the final temperature increase by 36.5% and temperature difference by 85.1%. The increase in cooling performance is likely due to the greater flow rate providing increased cooling capacity to the system, with more mass able to absorb heat each second, therefore maintaining the temperature gradient. However, increasing the coolant flow rate from 10 to 25 LPM saw limited additional cooling benefits, suggesting that the rate of heat transfer was no longer limited by the flow rate.

Additionally, Figure 13 suggests that greater C-rates increase temperature difference across a battery pack, with this decreasing slightly with an increase in flow rate. This is likely due to the increase in heat production and, therefore, overall pack temperatures. In turn, this would likely cause greater heat transfer to the coolant across the pack, reducing the temperature gradient at the coolant outlet, and thus reducing the rate of heat transfer from the end modules compared to those at the inlet.

4.2.2. Coolant Inlet Temperature

Figure 15 shows a positive relationship between coolant inlet temperature and thermal benefits, with correlation coefficients of 0.776 for cooling and 0.753 for heating obtained using the least-square method. Increased modification of the coolant temperature at extreme ambient temperatures would likely provide continued thermal benefits. However, due to the power demand associated with active coolant temperature modification, the BTMS should be optimised for each ambient temperature to minimise parasitic energy consumption. This can be achieved by implementing dynamic control of the thermal management system [57].

4.2.3. System Optimisation

Results shown in Section 3.3 and the CFD results [58] were used to optimise the BTMS. Figure 13 suggested that 18 LPM would be the optimal coolant flow rate per sub-pack, with this value found to be achievable in typical automotive applications [44]. This was determined by combining the point of diminishing returns, ~15 LPM, with a SF (safety factor) of 1.2. SFs of 1.2–1.5 have been suggested for battery systems [59], with 1.2 selected to minimise parasitic power consumption seen with increasing flow rates [37]. CFD results in [58] showed that at optimal ambient temperatures, ambient cooling would suffice. At extremes, it was found that an active system would be required, with 7.8 °C of active cooling or heating to be optimal [60].

4.3. Combined Transient Analysis Results

Figure 16 shows that the optimised cooling system demonstrated effective performance under ambient temperature conditions of 25 °C and 40 °C. When applied throughout the AVL drive cycle, the system enhanced the battery's thermal stability by 87.7% at 25 °C, ensuring the battery remained in the optimal temperature range for the entire drive cycle and 81% of the cycle at 40 °C.

This likely means that at ambient temperatures of 25 °C and above, the truck's battery would be thermally stable with the suggested parameters, avoiding issues like runaway, whilst achieving optimal performance on typical drive cycles.

Despite optimisation, Figure 16 showed poor BTMS performance at sub-zero temperatures, and the system's efficiency was not evaluated. These could likely be improved through the implementation of a battery preheating controller to improve low-temperature performance, with studies showing 40 °C temperature rises within an hour being possible [60]. This would allow the truck's battery to operate in its optimal temperature range with just 1 h of preheating. Studies have also shown that P.I.D style controllers can allow for reductions in operational time of BTMS during driving cycles, whilst maintaining thermal stability [61]. These could be used to reduce parasitic power draw, ultimately helping to improve battery range and BTMS efficiency.

5. Conclusions

This study develops a novel methodology, presenting the findings of an investigation into the electrical and thermal performance of a battery pack designed for a heavy-duty truck. The analysis employed 1D simulation techniques, utilising AVL CRUISE M and MATLAB Simulink Simscape R2023b, to evaluate the system under representative dynamic driving conditions. This approach allowed for a detailed assessment of energy consumption, state of charge (SoC), temperature fluctuations, and the effects of various cooling configurations while minimising computational costs. The simulations were conducted over two real-world drive cycles, providing valuable insights into the performance of the proposed battery pack design. The key findings of this investigation are as follows:

- As cell ageing progresses and the initial SoC decreases, the suitability of the battery pack for long-distance travel diminishes significantly, indicating that battery degradation plays a critical role in reducing range capabilities.
- Despite ageing, cells may exhibit improved range performance from regenerative braking during drive cycles, suggesting that drive cycle regeneration can partially offset the impacts of cell degradation.
- Increasing the coolant flow rate to 18 LPM and actively controlling the inlet temperature within ± 7.8 °C were found to significantly enhance thermal regulation, resulting in an 80%+ improvement in thermal stability under ambient conditions of 25 °C and 40 °C.
- The predicted single-charge range of the vehicle varied based on drive conditions, with a maximum range of 285 km, which underscores the variability in battery performance depending on real-world operating conditions.

The integration of AVL CRUISE M and MATLAB/Simulink Simscape R2023b in the simulations provided a comprehensive platform for both electrical and thermal analysis, offering a high degree of accuracy and flexibility. These tools were crucial in capturing the complex interactions between the battery pack's electrical behaviour and its thermal management system.

While this study's results offer a solid foundation for advancing electric propulsion systems in heavy-duty trucks, further design optimisation and experimental validation are needed. Future research should focus on validating the electrical and thermal performance of the proposed system through practical testing, incorporating parasitic power draws from auxiliary components such as pumps and compressors into the simulations, considering the effects of charging system behaviour, and developing a more robust BTMS tailored for electric heavy-duty vehicles. Also, higher C-rates should be considered for the analysis.

This investigation provides valuable insights into the performance and feasibility of battery packs in heavy-duty electric trucks, especially concerning their thermal and electrical characteristics in dynamic driving conditions. This study highlights the need for further cooling optimisation and increased battery longevity. As electric mobility continues

to evolve, this research will contribute to the goal of achieving more sustainable and efficient heavy-duty electric vehicles.

Author Contributions: M.M.: Conceptualisation, Methodology, Investigation, Formal Analysis, Validation, Software, Writing—Original Draft, and Data Curation; T.S.: Conceptualisation, Methodology, Investigation, Formal Analysis, Validation, Software, Writing—Original Draft, and Data Curation; U.T.: Investigation, Formal Analysis, Software, Writing—Original Draft, and Data Curation; F.S.: Conceptualisation, Methodology, Supervision, and Writing—Review and Editing; H.T.: Writing—Review and Editing, and Supervision; M.B.: Conceptualisation, Methodology, Software, Supervision, and Writing—Review and Editing. All authors have read and agreed to the published version of the manuscript.

Funding: This research received no external funding.

Data Availability Statement: The original data presented in the study are included in the article, and further inquiries can be directed to the corresponding author.

Acknowledgments: The authors acknowledge AVL List GmbH's support for providing the simulation tools for the University of Leeds through their University Partnership Programme is appreciated.

Conflicts of Interest: Author Farhad Salek was employed by the company AVL Powertrain UK Limited. The remaining authors declare that the research was conducted in the absence of any commercial or financial relationships that could be construed as a potential conflict of interest.

References

1. Hansen, J.; Ruedy, R.; Sato, M.; Lo, K. Global surface temperature change. *Rev. Geophys.* **2010**, *48*, RG000345. [CrossRef]
2. Hannah, R. Cars, Planes, Trains: Where Do CO_2 Emissions from Transport Come from? Our World in Data. 2020. Available online: https://ourworldindata.org/co2-emissions-from-transport (accessed on 14 April 2024).
3. European Parliament. Regulation (EU) 2019/631 of the European Parliament and of the Council of 17 April 2019 setting CO_2 emission performance standards for new passenger cars and for new light commercial vehicles, and repealing Regulations (EC) No 443/2009 and (EU) No 510/2011. *Off. J. Eur. Union* **2021**, *L 111*, 13–53.
4. Department of Transport, Government Takes Historic Step Towards Net-Zero with End of Sale of New Petrol and Die-Sel Cars by 2030. 2020. Available online: https://www.gov.uk/government/news/government-takes-historic-step-towards-net-zero-with-end-of-sale-of-new-petrol-and-diesel-cars-by-2030 (accessed on 15 April 2024).
5. Abnett, K. Electric Car Sales Surge as Europe's Climate Targets Bite. 2021. Available online: https://www.reuters.com/business/sustainable-business/electric-car-sales-surge-europes-climate-targets-bite-2021-06-29/ (accessed on 16 April 2024).
6. Thomas, C.E.S. Transportation options in a carbon-constrained world: Hybrids, plug-in hybrids, biofuels, fuel cell electric vehicles, and battery electric vehicles. *Int. J. Hydrogen Energy* **2009**, *34*, 9279–9296. [CrossRef]
7. Department for Transport. UK Confirms Pledge for Zero-Emission HGVs by 2040 and Unveils New Chargepoint Design. 2021. Available online: https://www.gov.uk/government/news/uk-confirms-pledge-for-zero-emission-hgvs-by-2040-and-unveils-new-chargepoint-design#:~:text=News%20story-,UK%20confirms%20pledge%20for%20zero-emission%20HGVs%20by%202040%20and,within%20the%20next%202%20decades.&text=All%20new%20heavy%20goods%20vehicles,today%20(10%20November%202021) (accessed on 20 November 2024).
8. Hao, H.; Geng, Y.; Tate, J.E.; Liu, F.; Chen, K.; Sun, X.; Liu, Z.; Zhao, F. Impact of transport electrification on critical metal sustainability with a focus on the heavy-duty segment. *Nat. Commun.* **2019**, *10*, 5398. [CrossRef]
9. Agency, I.E. Global EV Outlook 2021: Accelerating Ambitions Despite the Pandemic. 2021. Available online: www.iea.org/t&c/ (accessed on 15 April 2024).
10. Transport, D.O. A Simplified Guide to Lorry Types and Weights. 2023. Available online: https://assets.publishing.service.gov.uk/media/5a74dbd340f0b65f61322ceb/simplified-guide-to-lorry-types-and-weights.pdf (accessed on 16 April 2024).
11. Hasnain, A.; Gamwari, A.S.; Resalayyan, R.; Sadabadi, K.F.; Khaligh, A. Medium and heavy duty vehicle electrification: Trends and technologies. *IEEE Trans. Transp. Electrif.* **2024**. [CrossRef]
12. Sandeep, V.; Shastri, S.; Sardar, A.; Salkuti, S.R. Modeling of battery pack sizing for electric vehicles. *Int. J. Power Electron. Drive Syst.* **2020**, *11*, 1987–1994. [CrossRef]
13. Salek, F.; Morrey, D.; Henshall, P.; Resalati, S. *Techno-Economic Assessment of Utilising Second-Life Batteries in Electric Vehicle Charging Stations*; SAE: Warrendale, PA, USA, 2023. [CrossRef]

14. Tudoroiu, R.E.; Zaheeruddin, M.; Tudoroiu, N.; Radu, S.M. SOC estimation of a rechargeable li-ion battery used in fuel cell hybrid electric vehicles—Comparative study of accuracy and robustness performance based on statistical criteria. Part II: SOC estimators. *Batteries* **2020**, *6*, 41. [CrossRef]
15. Basma, H.; Beys, Y.; Rodríguez, F. Battery Electric Tractor-Trailers in the European Union: A Vehicle Technology Analysis. 2021. Available online: www.theicct.org (accessed on 15 April 2024).
16. Yao, L.W.; Aziz, J.A.; Kong, P.Y.; Idris, N.R.N. Modeling of lithium-ion battery using MATLAB/simulink. In Proceedings of the IECON 2013—39th Annual Conference of the IEEE Industrial Electronics Society, Vienna, Austria, 10–13 November 2013; pp. 1729–1734.
17. Salek, F.; Azizi, A.; Resalati, S.; Henshall, P.; Morrey, D. Mathematical modelling and simulation of second life battery pack with heterogeneous state of health. *Mathematics* **2022**, *10*, 3843. [CrossRef]
18. Martyushev, N.V.; Malozyomov, B.V.; Sorokova, S.N.; Efremenkov, E.A.; Qi, M. Mathematical modeling of the state of the battery of cargo electric vehicles. *Mathematics* **2023**, *11*, 536. [CrossRef]
19. Pesaran, A.A. Battery thermal models for hybrid vehicle simulations. *J. Power Sources* **2002**, *110*, 370–382. [CrossRef]
20. Pesaran, A.; Santhanagopalan, S.; Kim, G.H. *Addressing the Impact of Temperature Extremes on Large Format Li-Ion Batteries for Vehicle Applications (Presentation)*; National Renewable Energy Lab.(NREL): Golden, CO, USA, 2013.
21. Tarascon, J.-M.; Gozdz, A.S.; Schmutz, C.; Shokoohi, F.; Warren, P.C. Performance of Bellcore's plastic rechargeable Li-ion batteries. *Solid State Ion.* **1996**, *86*, 49–54. [CrossRef]
22. Lo, J. Effect of Temperature on Lithium-Iron Phosphate Battery Performance and Plug-In Hybrid Electric Vehicle Range. Master of Applied Science Thesis, University of Waterloo, Waterloo, ON, USA, 2013.
23. Kim, J.; Oh, J.; Lee, H. Review on battery thermal management system for electric vehicles. *Appl. Therm. Eng.* **2019**, *149*, 192–212. [CrossRef]
24. Choudhari, V.G.; Dhoble, D.A.S.; Sathe, T.M. A review on effect of heat generation and various thermal management systems for lithium ion battery used for electric vehicle. *J. Energy Storage* **2020**, *32*, 101729. [CrossRef]
25. Greco, A.; Cao, D.; Jiang, X.; Yang, H. A theoretical and computational study of lithium-ion battery thermal management for electric vehicles using heat pipes. *J. Power Sources* **2014**, *257*, 344–355. [CrossRef]
26. Saw, L.H.; Ye, Y.; Tay, A.A.O.; Chong, W.T.; Kuan, S.H.; Yew, M.C. Computational fluid dynamic and thermal analysis of Lithium-ion battery pack with air cooling. *Appl. Energy* **2016**, *177*, 783–792. [CrossRef]
27. Tesla, Dimensions and Weights. 2024. Available online: https://www.tesla.com/ownersmanual/model3/en_cn/GUID-56562137-FC31-4110-A13C-9A9FC6657BF0.html (accessed on 13 November 2024).
28. Nissan. Leaf, the Electric Family Car. 2024. Available online: https://www.nissan.co.uk/vehicles/new-vehicles/leaf.html?cid=psm_cmid=17064511648_grid=131231644970_adid=595105867889&gad_source=1&gclid=CjwKCAiAudG5BhAREiwAWMlSjF4SKaC72zA2ccqbWAoHdD7rTwQSaUZfqC8-JupvA95B2gdF-CqO1BoCtvAQAvD_BwE&gclsrc=aw.ds (accessed on 13 November 2024).
29. Volvo. FH Specifications. 2024. Available online: https://www.volvotrucks.co.uk/en-gb/trucks/models/volvo-fh/specifications.html (accessed on 13 November 2024).
30. Gunes, F.; Yang, Y.; Kim, B.; Wellers, M. Mechanical hybrid control for heavy-goods vehicle. In Proceedings of the 2018 UKACC 12th International Conference on Control, Sheffield, UK, 5–7 September 2018; pp. 127–132. [CrossRef]
31. Singh, A.K.; Dalai, A.; Kumar, P. Analysis of induction motor for electric vehicle application based on drive cycle analysis. In Proceedings of the 2014 IEEE International Conference on Power Electronics, Drives and Energy Systems, Mumbai, India, 16–19 December 2014; pp. 1–6. [CrossRef]
32. Salameh, M.; Brown, I.P.; Krishnamurthy, M. Fundamental evaluation of data clustering approaches for driving cycle-based machine design optimization. *IEEE Trans. Transp. Electrif.* **2019**, *5*, 1395–1405. [CrossRef]
33. Leonard, A.T.; Salek, F.; Azizi, A.; Resalati, S. Electrification of a class 8 heavy-duty truck considering battery pack sizing and cargo capacity. *Appl. Sci.* **2022**, *12*, 9683. [CrossRef]
34. Pesaran, A. Battery thermal management in EVs and HEVs: Issues and solutions. In Proceedings of the Advanced Automotive Battery Conference, Las Vegas, NV, USA, 6–8 February 2001; p. 10.
35. Xu, X.; Li, W.; Xu, B.; Qin, J. Numerical study on a water cooling system for prismatic LiFePO4 batteries at abused operating conditions. *Appl. Energy* **2019**, *250*, 404–412. [CrossRef]
36. Piao, C.; Chen, T.; Zhou, A.; Wang, P.; Chen, J. Research on electric vehicle cooling system based on active and passive liquid cooling. *J. Phys. Conf. Ser.* **2020**, *1549*, 042146. [CrossRef]
37. Lan, C.; Xu, J.; Qiao, Y.; Ma, Y. Thermal management for high power lithium-ion battery by minichannel aluminum tubes. *Appl. Therm. Eng.* **2016**, *101*, 284–292. [CrossRef]
38. Karimi, D.; Behi, H.; Hosen, M.S.; Jaguemont, J.; Berecibar, M.; Van Mierlo, J. A compact and optimized liquid-cooled thermal management system for high power lithium-ion capacitors. *Appl. Therm. Eng.* **2020**, *185*, 116449. [CrossRef]

39. Yue, Q.L.; He, C.X.; Wu, M.C.; Xu, J.B.; Zhao, T.S. Pack-level modeling of a liquid cooling system for power batteries in electric vehicles. *Int. J. Heat Mass Transf.* **2022**, *192*, 122946. [CrossRef]
40. Broatch, A.; Olmeda, P.; Margot, X.; Agizza, L. A generalized methodology for lithium-ion cells characterization and lumped electro-thermal modelling. *Appl. Therm. Eng.* **2022**, *217*, 119174. [CrossRef]
41. Samsung. *Introduction of Samsung SDI's 94 Ah Cells*. 2015. Available online: https://files.gwl.eu/inc/_doc/attach/StoItem/7213/30118_Introduction%20of%20SDI%20EV%2094Ah%20cell_V9-2.pdf (accessed on 12 November 2024).
42. Wang, Q.; Jiang, B.; Li, B.; Yan, Y. A critical review of thermal management models and solutions of lithium-ion batteries for the development of pure electric vehicles. *Renew. Sustain. Energy Rev.* **2016**, *64*, 106–128. [CrossRef]
43. Boyd, J. China and Japan push for a global charging standard for EVs. *IEEE Spectr.* **2018**, *56*, 12–13. [CrossRef]
44. Vovyo Pump, Automotive Electric Water Pump. 2024. Available online: https://www.vovyopump.com/automotive-electric-water-pump/ (accessed on 15 April 2024).
45. Hoşöz, M.; Gündem, A.; Keklik, E. Performance comparison of propylene glycol-water and ethylene glycol-water mixtures as engine coolants in a flat-tube automobile radiator. *Int. J. Automot. Sci. Technol.* **2021**, *5*, 147–156. [CrossRef]
46. Mathworks. Battery: Generic Battery Model; n.d. Available online: https://uk.mathworks.com/help/sps/powersys/ref/battery.html (accessed on 12 November 2024).
47. Lai, X.; Gao, W.; Zheng, Y.; Ouyang, M.; Li, J.; Han, X.; Zhou, L. A comparative study of global optimization methods for parameter identification of different equivalent circuit models for Li-ion batteries. *Electrochim. Acta* **2019**, *295*, 1057–1066. [CrossRef]
48. Zhang, A.; Li, Y. Thermal conductivity of aluminum alloys—A review. *Materials* **2023**, *16*, 2972. [CrossRef]
49. ANSYS Inc. *ANSYS Fluent Theory Guide*; ANSYS Inc.: Canonsburg, PA, USA, 2023.
50. Mazhar, S.; Qarni, A.A.; Haq, Y.U.; Haq, Z.U.; Murtaza, I. Promising PVC/MXene based flexible thin film nanocomposites with excellent dielectric, thermal and mechanical properties. *Ceram. Int.* **2020**, *46*, 12593–12605. [CrossRef]
51. Dow Chemical Company. Engineering and Operating Guide for Dowfrost and Dowfrost HD inhibited Propylene Glycol-Based Heat Transfer Fluids. 2008. Available online: https://www.dow.com/documents/180/180-01286-01-engineering-and-operating-guide-for-dowfrost-and-dowfrost-hd.pdf?iframe=true#:~:text=Composition%20(%25%20by%20weight)%20Propylene%20Glycol%2095.5%2094.0,10.7%20Reserve%20Alkalinity%20(min.)%209.0%20ml%2016.0%20ml (accessed on 12 November 2024).
52. MathWorks. MATLAB Simulink. 2023. Available online: https://www.mathworks.com/ (accessed on 4 December 2024).
53. Durst, F.; Arnold, I. *Fluid Mechanics: An Introduction to the Theory of Fluid Flows*; Springer: Berlin/Heidelberg, Germany, 2008.
54. Salek, F.; Halder, P.; Leonard, A.T.; Babaie, M.; Resalati, S.; Zare, A. *Battery Sizing, Parametric Analysis, and Powertrain Design for a Class 8 Heavy-Duty BATTERY Electric Truck*; SAE Technical Paper Series; SAE: Warrendale, PA, USA, 2023. Available online: https://api.semanticscholar.org/CorpusID:258034060 (accessed on 12 November 2024).
55. Salek, F.; Abouelkhair, E.; Babaie, M.; Cunliffe, F.; Zare, A. Assessment of the powertrain electrification for a heavy-duty class 8 truck for two different electric drives. In Proceedings of the SAE Powertrains, Fuels & Lubricants Conference & Exhibition, Krakow, Poland, 6–8 September 2022; p. 8.
56. DAF. New Generation DAF Electric. 2024. Available online: https://www.daf.co.uk/en-gb/trucks/new-generation-daf-electric (accessed on 17 November 2024).
57. Kim, E.; Shin, K.G.; Lee, J. Real-time battery thermal management for electric vehicles. In Proceedings of the 2014 ACM/IEEE International Conference on Cyber-Physical Systems (ICCPS), Berlin, Germany, 14–17 April 2014; pp. 72–83. [CrossRef]
58. Makings, M.; Maciocha, M.; Biggs, J.; Salek, F.; Zare, A.; Resalati, S.; Short, T.; Babaie, M. *CFD Analysis of the Battery Thermal Management System for a Heavy-Duty Truck*; WCX SAE World Congress Experience; SAE Technical Paper; SAE: Warrendale, PA, USA, 2024. [CrossRef]
59. Henke, M.; Hailu, G. Thermal management of stationary battery systems: A literature review. *Energies* **2020**, *13*, 4194. [CrossRef]
60. Wu, S.; Xiong, R.; Li, H.; Nian, V.; Ma, S. The state of the art on preheating lithium-ion batteries in cold weather. *J. Energy Storage* **2020**, *27*, 101059. [CrossRef]
61. Angermeier, S.; Ketterer, J.; Karcher, C. Liquid-based battery temperature control of electric buses. *Energies* **2020**, *13*, 4990. [CrossRef]